JOURNAL OF THEORETICAL AND APPLIED MECHANICS
46, 4, pp. 879-896, Warsaw 2008

CHAOTIC VIBRATIONS IN GEAR MESH SYSTEMS

Jan Łuczko

Cracow University of Technology, Institute of Applied Mechanics, Cracow, Poland
e-mail: jluczko@mech.pk.edu.pl

The paper is concerned with qualitative analysis of a non-linear model describing vibrations of a gear mesh system. The influence of selected parameters on the character and level of vibrations is studied.
The possibility of excitation of quasi-periodic or chaotic oscillations for some regions of the parameters has been shown. Different types of vibration are illustrated by plots of time histories, phase portraits, stroboscopic portraits and bifurcation diagrams.

Key words: non-linear vibration, chaos, gear

1. Introduction

Dynamic models of gear mesh systems are most often described by non-linear parametrical equations, i.e. differential equations with time-periodic coefficients (Müller, 1986; Dyk *et al.*, 1994; Raghothama and Narayanan, 1999; Theodossiades and Natsiavas, 2001; Litak and Friswell, 2003). The variability of coefficients results in variation of the meshing stiffness induced mainly by a change of the number of gear teeth pairs, which are simultaneously in contact (meshing of one or two pairs of teeth). The nonlinearity of equations is the result of backlashes in the transmission gear. Impacts of teeth are the effect of backlashes, and characteristics of impacts forces are strongly non-linear. As a result of these impact forces, it is possible, under some conditions, for periodic, quasi-periodic or chaotic vibration to occur in the system.

Main sources of vibrations are kinematic excitations caused by manufacturing errors and wear. Frequencies of such excitations depend on the product of rotational speed and the number of teeth. Non-linear characteristics of the driving moment, dependent on rotation angles and angular speed are sometimes taken into account.

In the literature, a simplified one degree-of-freedom model is usually used where the torsional stiffnesses of shafts as well as transverse vibrations are neglected. In this classical model, the gear mesh is modelled as a pair of rigid disks connected by a spring-damper set along the line of action. The backlash function is usually used to represent gear clearances and an external displacement excitation is also applied at the gear mesh interface to represent manufacturing errors, intentional modifications of teeth or wear profile. The most of existing models of gear transmission systems treat the gear errors as a deterministic input.

Another one-stage gearbox model was presented by Müller (1986). This model attracted a lot of attention in Poland. Müller's model is a two-parameter (stiffness and damping) one in which the inertia of two gear wheels is reduced to one mass. It was discussed, for example, in the paper by Dyk *et al.* (1994). Motion of the mass is equivalent to relative motion of two gear wheels. Vibration is caused by relative motion of springs (having different lengths) which are in contact with the mass.

In the paper by Dyk *et al.* (1994), a comparison between the results of the analysis by the classical and Müller's model was presented. The comparison showed that chaotic vibration can be observed in the case when the parameters of the model differ from those existing in a real construction.

Raghothama and Narayanan (1999) investigated coupled transverse and torsional vibrations of a geared rotor-bearing system using the classical model. Periodic motions were obtained by the incremental harmonic balance method. The path following procedure using the arc length continuation technique was then used to trace bifurcation diagrams.

A similar approach to the analysis of periodic vibrations was presented by Theodossiades and Natsiavas (2001) who studied the influence of gear meshing frequency on the steady state response curve.

Some models additionally include effects of friction between gear teeth. For example, in the paper by Vaishya and Singh (2001), the influence of sliding friction and viscous damping on unstable regions was discussed.

The phenomenon of chaotic vibrations in gear transmission systems has been relatively early detected. Usually, strange attractors are shown only for suitably chosen values of gearbox parameters. In some papers, bifurcation diagrams were calculated to determine ranges of chaotic vibrations (e.g., Li *et al.*, 2001).

Taking into account the torsional stiffness, one needs to study a three degrees-of-freedom model. Litak and Friswell (2003) showed diagrams obtained by numerical integration, which illustrate the influence of the shaft stiffness as well as the magnitude of excitation on the character of motion.

The coefficient of restitution has been also used to describe the impacts of teeth. In the paper by De Souza *et al.* (2004) in order to illustrate the influence of this coefficient on the type of vibration, the authors determined the bifurcation diagram as well as they calculated the Lyapunov exponents.

Recently, the interest towards developing a better understanding of gear vibration has been renewed. This interest has been clearly reflected in some new studies which have dealt with a relatively simple model with rigid supports. Analysing this model by the harmonic balance method (e.g., Shen *et al.*, 2006) as well as the method of numerical integration (e.g., Gill-Jeong, 2007), the authors investigated the influence of selected parameters on frequency-response curves. A similar model, in which manufacturing errors were treated stochastically, was investigated by Bonori and Pellicano (2007).

In the present paper, a four-degree-of-freedom model with the backlash and time varying stiffness is used to describe vibration of a one-stage gearbox. The influence of significant parameters on the character of vibration and the quality criteria are presented. Two-parameter diagrams are obtained to provide a better description of dynamic behaviour of the system. The study is done numerically using methods of numerical integration and spectrum analysis (Łuczko, 2006).

2. The model of the system

A pair of gears is modelled (Fig. 1) using two disks coupled by a non-linear mesh stiffness (parameters c, Δ) and a linear mesh damping (coefficient k). It is assumed that the resilient elements of the supports are described by the Voigt-Kelvin model with damping coefficients k_1 and k_2 and stiffness coefficients c_1 and c_2. Motion of the system is described by rotational angles φ_1 and φ_2 and displacements u_1 and u_2 of the centers of the disks. The model takes into account the influence of torques M_1 and M_2 on the driving and driven shaft, respectively.

Using the laws of momentum and angular momentum, transverse-torsional motion of the system can be described by the following system of four second-order differential equations

$$\begin{aligned} &I_1\ddot{\varphi}_1 + R_1 S = M_1(\dot{\varphi}_1, \varphi_1, t) && I_2\ddot{\varphi}_2 - R_2 S = -M_2(\dot{\varphi}_2, \varphi_2, t) \\ &m_1\ddot{u}_1 + k_1\dot{u}_1 + c_1 u_1 + S = 0 && m_2\ddot{u}_2 + k_2\dot{u}_2 + c_2 u_2 - S = 0 \end{aligned} \tag{2.1}$$

In equations (2.1), the parameters: m_1, m_2 and I_1, I_2 are, respectively, the gear masses and the mass moments of inertia of the gears about their

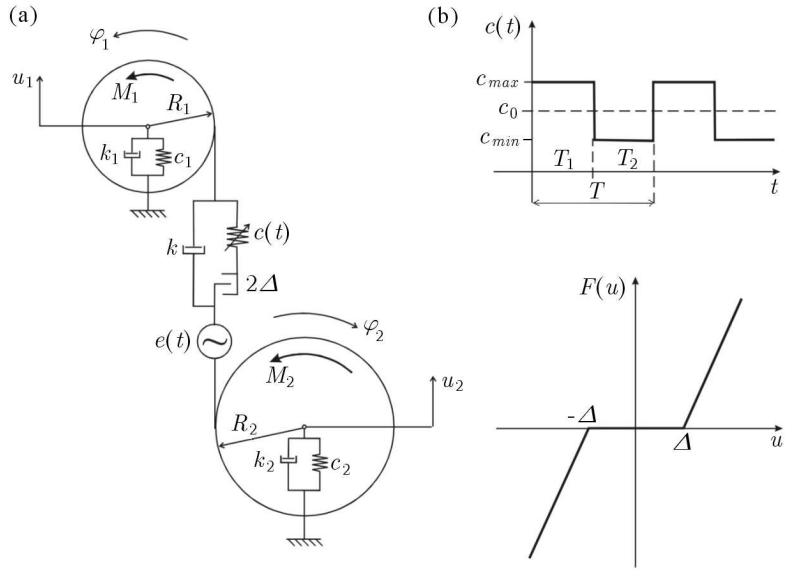

Fig. 1. A gear pair: (a) model of the system, (b) characteristics $c(t)$ and $F(u)$

axis of symmetry. The base radii of the gears are denoted by R_1 and R_2. The meshing force S is normal to the involute profile of the gear tooth. The following relationships for the torques M_1 and M_2 are used in the model

$$M_1(\dot{\varphi}_1, \varphi_1, t) = M_{10} - b_1\dot{\varphi}_1 \qquad M_2(\dot{\varphi}_2, \varphi_2, t) = M_{20} - b_2\dot{\varphi}_2 \tag{2.2}$$

where b_1 and b_2 are the damping coefficients in the journal bearings.

The meshing force S depends on the relative displacement of gear teeth, which describes the so-called dynamic transmission error

$$u = R_1\varphi_1 - R_2\varphi_2 + u_1 - u_2 - e(t) \tag{2.3}$$

In equation (2.3), the so-called static transmission error e(t) takes into account the effects of gear faults such as wear of the tooth face, mount error, tooth spall, etc. This error depends on the rotational angles φ_1 and φ_2. However, in this case, the influence of torsional vibrations on the rotational speed is usually neglected and the static error $e(t)$ depends directly on time. Introducing the notation $\omega_z = n_1\omega_1 = n_2\omega_2$ for the fundamental frequency (gear meshing frequency), the static transmission error can be expressed in the form of a Fourier series

$$e(t) = \sum_j e_j \cos(j\omega_z t - \theta_j) \tag{2.4}$$

where the integers n_1 and n_2 stand for the number of teeth of each gear.

The meshing force S is given by the following formula

$$S = k\dot{u} + c(t)F(u) \tag{2.5}$$

The gear backlash nonlinearity $F(u)$ is modelled as a piecewise linear function

$$F(u) = \begin{cases} u - \Delta & \text{for} \quad u > \Delta \\ 0 & \text{for} \quad |u| \leqslant \Delta \\ u + \Delta & \text{for} \quad u < -\Delta \end{cases} \tag{2.6}$$

where 2Δ is the backlash. The stiffness $c(t)$ depends on the number and position of the gear teeth pairs which are in contact. It is a periodic function of the relative angular position of the gears. The function $c(t)$ has a similar form as equation (2.5) discussed earlier

$$c(t) = \sum_j c_j \cos(j\omega_z t - \alpha_j) \tag{2.7}$$

or it takes a characteristic shown in Fig. 1b. This somewhat idealized characteristic takes into account the change of stiffness only due to the change of the number of teeth which are in contact. The periods T_1 and T_2, in which one or two pairs of teeth are in contact, can be expressed by the profile contact ratio α in the following way: $T_1 = (\alpha - 1)T$ and $T_2 = (2 - \alpha)T$, where $T = 2\pi/\omega_z$.

The analysis will be done in a dimensionless form, and non-dimensional quantities are used where the displacements are referred to the parameter Δ and the non-dimensional time $\tau = \omega_0 t$ is connected with the circular frequency

$$\omega_0 = \sqrt{\frac{c_0}{m}} \tag{2.8}$$

where

$$m = \frac{I_1 I_2}{I_1 R_2^2 + I_2 R_1^2} \tag{2.9}$$

is the equivalent mass representing the total inertia of a gear pair. Introducing new variables $(n = 1, 2)$

$$x_n = r_n \varphi_n = \frac{R_n}{\Delta}\varphi_n \qquad y_n = \frac{1}{\Delta}u_n \tag{2.10}$$

and following notations

$$
\begin{aligned}
&J_n = \frac{I_n}{mR_n^2} \qquad && \mu_n = \frac{m_n}{m} \qquad && q_n = \frac{M_{n0}}{c_0 R_n \Delta} \\
&\varepsilon_j = \frac{e_j}{\Delta} \qquad && \zeta_n = \frac{k_n}{2m_n\omega_0} \qquad && \zeta = \frac{k}{2m\omega_0} \\
&\beta_n = \frac{b_n}{2m\omega_0 R_n^2} \qquad && \kappa_n = \frac{c_n}{c_0}
\end{aligned}
\tag{2.11}
$$

the differential equations assume the following dimensionless form

$$
\begin{aligned}
&J_1\frac{d^2x_1}{d\tau^2} + 2\beta_1\frac{dx_1}{d\tau} + 2\zeta\frac{dz}{d\tau} + \chi(\tau)f(z) = q_1 \\
&J_2\frac{d^2x_2}{d\tau^2} + 2\beta_2\frac{dx_2}{d\tau} - 2\zeta\frac{dz}{d\tau} - \chi(\tau)f(z) = q_2 \\
&\mu_1\frac{d^2y_1}{d\tau^2} + 2\mu_1\zeta_1\frac{dy_1}{d\tau} + \kappa_1 y_1 + 2\zeta\frac{dz}{d\tau} + \chi(\tau)f(z) = 0 \\
&\mu_2\frac{d^2y_2}{d\tau^2} + 2\mu_2\zeta_2\frac{dy_2}{d\tau} + \kappa_2 y_2 - 2\zeta\frac{dz}{d\tau} - \chi(\tau)f(z) = 0
\end{aligned}
\tag{2.12}
$$

Here

$$
f(z) = \begin{cases} z-1 & \text{for} \quad z > 1 \\ z+1 & \text{for} \quad |z| \leqslant 1 \\ z+1 & \text{for} \quad z < -1 \end{cases}
\tag{2.13}
$$

where

$$
z = x_1 - x_2 + y_1 - y_2 - \varepsilon(t)
\tag{2.14}
$$

and

$$
\varepsilon(t) = \sum_j \varepsilon_j \cos(j\omega\tau - \theta_j)
\tag{2.15}
$$

For the characteristic shown in Fig. 1b, the function $\chi(\tau)$ in the interval $(0, 2\pi/\omega)$, where $\omega = \omega_z/\omega_0$, has the following form

$$
\chi(\tau) = \begin{cases} 1+\chi_1 & \text{for} \quad 0 \leqslant \tau < \tau_1 \\ 1-\chi_2 & \text{for} \quad \tau_1 \leqslant \tau < \tau_1 + \tau_2 \end{cases}
\tag{2.16}
$$

In the case of a fixed support ($\kappa_1 \to \infty$, $\kappa_2 \to \infty$, $y_1 = y_2 = 0$), and using an additional assumption that $\beta_1 = \beta_2 = 0$, vibrations of the gear mechanism can be described by the following differential equation

$$
\frac{d^2z}{d\tau^2} + 2\zeta_0\frac{dz}{d\tau} + \chi_0(\tau)f(z) = q_0 - \frac{d^2\varepsilon}{d\tau^2}
\tag{2.17}
$$

where

$$\chi_0(\tau) = \frac{J_1 + J_2}{J_1 J_2}\chi(\tau) \qquad \zeta_0 = \frac{J_1 + J_2}{J_1 J_2}\zeta$$
$$q_0 = \frac{q_1}{J_1} + \frac{q_2}{J_2} \tag{2.18}$$

3. Analysis of torsional vibrations

Some results of qualitative analysis will be described below. The results have been obtained using methods of numerical integration and the Fast Fourier Transform. More details about the use of spectrum analysis for determination of the character of vibration were discussed in Łuczko (2006).

In the discussion of the results, the criterion index V_{RMS} is used, defined as the velocity rms value. Moreover, it has also been assumed that $J_1 = J_2 = 2$ and $q_1 = q_2$, so that the following relationships take place: $\chi_0(\tau) = \chi(\tau)$, $\zeta_0 = \zeta$ and $q_0 = q_1 = q_2$. The following set values of parameters have been used in the numerical calculations: $\zeta = 0.025$, $\beta_1 = \beta_2 = 0.01$, $\chi_1 = \chi_2 = \chi_0 = 0.25$, $\theta_1 = 0$ and $\alpha = 1.5$ (then $T_1 = T_2 = T/2$).

We begin the study of equations (2.12) by analysing torsional vibrations, neglecting the transverse displacements u_1 and u_2. In this case, motion is described by the first two equations of (2.12) or equation (2.17) for $\beta_1 = \beta_2 = 0$.

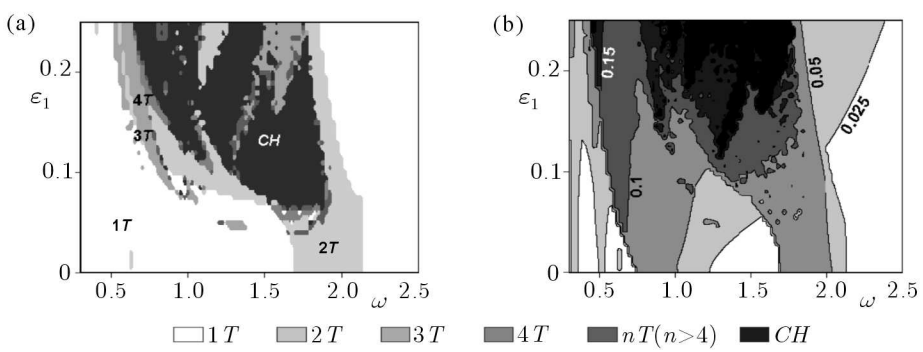

Fig. 2. Influence of the excitation frequency and amplitude ($\chi_0 = 0.25$, $q_0 = 0.1$, $\theta_1 = 0$, $\zeta = 0.025$) on: (a) vibration zones, (b) efficiency index

Figure 2 illustrates the influence of the frequency ω and amplitude ε_1 of the first harmonic of the excitation on the character of vibration as well

as on the rms value of the velocity (efficiency index). In the lower frequency range (for $\omega < 2$), apart from periodic vibrations, interesting sub-harmonic (most often $2T$-periodic) and chaotic vibrations can be observed. The regions of chaotic vibrations have irregular shapes (Fig. 2a) and the changes of the efficiency index (Fig. 2b) in these regions are also irregular. Additionally, the level of vibration (measured by the introduced index) is usually somewhat higher, but it is not a general rule.

The raised level of vibration is also observed in the regions of parametrical resonance. These regions begin in the neighbourhoods of points $\omega = 2$, $\omega = 1$, $\omega = 1/2$ and $\omega = 1/4$, which is typical for parametric vibration. The widest are the first two regions. In these regions too, for a large enough amplitude ε_1, chaotic vibrations are induced very often.

For the determination of solutions to equations (2.12), the following initial conditions were used: $x_2(0) = x_1'(0) = x_2'(0) = 0$, $x_1(0) = 1$. The condition $x_1(0) = 1$ means that at the time $t = 0$, the contact takes place between the meshing teeth and the force acting on the gear tooth causes revolution in the direction consistent with the assumed direction of the angular velocity of the driven shaft.

For other initial conditions, the results are similar, however sometimes, especially for a smaller excitation amplitude (in the vicinity of the boundary of the regions) more solutions are observed. A more exact analysis of the influence of the initial conditions on the character of vibration requires determination of the basins of attraction.

In the case of a system with four degrees-of-freedom, one needs to analyse the influence of four initial conditions. This is arduous calculation and, additionally, the results are difficult to illustrate graphically in that case.

Because the influence of the parameters β_1 and β_2 (damping in the bearings) on the shape of the determined regions is insignificant, it is possible to find the basins of attraction by analysing the simpler system described by equation (2.17).

The results of analysis of the influence of initial conditions on the solution to equation (2.17) are shown in Fig. 3. For smaller values of the frequency, two different types of vibrations get mostly excited (Figs. 3a,b). For larger values of ω, the number of solutions grows drastically (Fig. 3c). For instance, in the case of $\omega = 2.3$ and $\varepsilon_1 = 0.05$, one can show the existence, apart from $1T$-periodic vibration (Fig. 4a) and $3T$-periodic (Fig. 4b), two types of $4T$-periodic vibration (Figs. 4c,d). Additionally, for a small change in the parameters ω and ε_1, $5T$-periodic vibrations appear in the system.

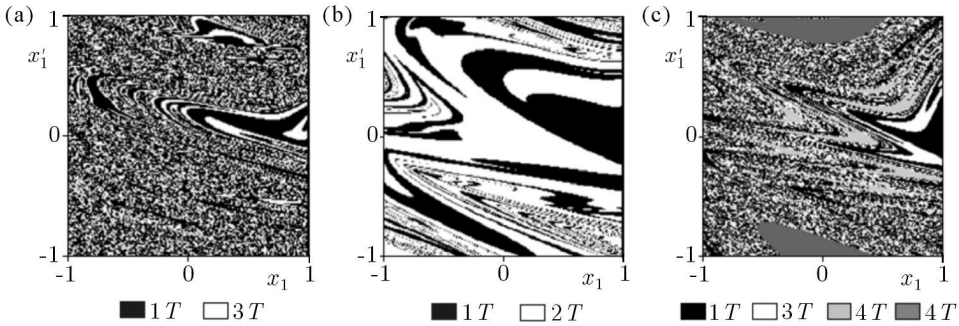

Fig. 3. Basins of attraction ($\chi = 0.25$, $q_0 = 0.1$, $\zeta = 0.025$): (a) $\omega = 0.8$, $\varepsilon_1 = 0.1$, (b) $\omega = 1.1$, $\varepsilon_1 = 0.05$, (c) $\omega = 2.3$, $\varepsilon_1 = 0.05$

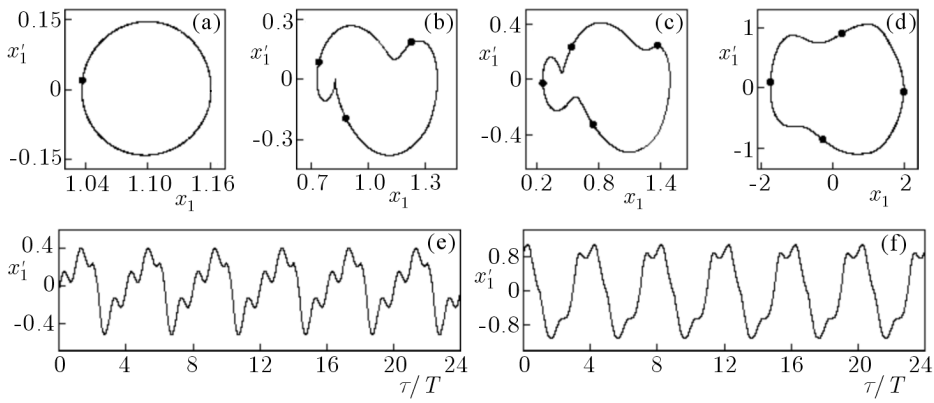

Fig. 4. Phase trajectories and time histories of the velocity ($\omega = 2.3$, $\varepsilon_1 = 0.05$): (a) $1T$-periodic, (b) $2T$-periodic, (c), (e) $4T$-periodic, (d), (f) $4T$-periodic

The frequency ω and amplitude ε_1 of the kinematic excitation as well as undimensional torque q_0 have the biggest influence on the character of vibration. The influence of parametric excitation $(\chi_1, \chi_2, \tau_1, \tau_2)$ is considerably smaller. Very similar results are obtained, by replacing the function $\chi(\tau)$, defined by formula (2.16), with a sine function having a suitably chosen amplitude. The parameters χ_1 and χ_2 mainly influence the velocity rms value.

Figure 5 illustrates, in the same format as in Fig. 2, the effect of ω and q_0 (static load torque). Chaotic vibrations are excited for small values of q_0 (for $q_0 < 0.15$).

With an increase in q_0, the range of chaotic vibrations strongly decreases (Fig. 5a), however the range of $2T$-periodic vibration simultaneously increases. Other types of sub-harmonic vibration are mainly observed on the boundary of zones of different vibration types.

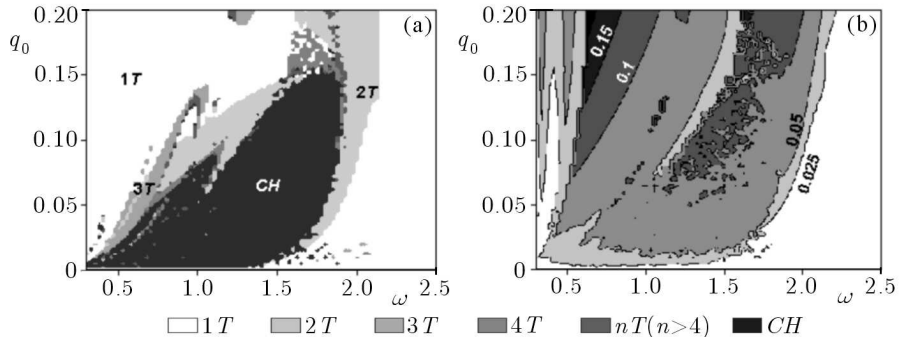

Fig. 5. Effect of ω and q_0 ($\chi_0 = 0.25$, $\varepsilon_1 = 0.1$, $\zeta = 0.025$): (a) vibration zones, (b) quality index

In the regions of periodic vibration, the changes of quality index are regular (Fig. 5b). With an increase in q_0, in some frequency ranges, the level of vibrations slightly increased. The quality index achieves small values for higher values of ω (for $\omega > 2$), independently of q_0.

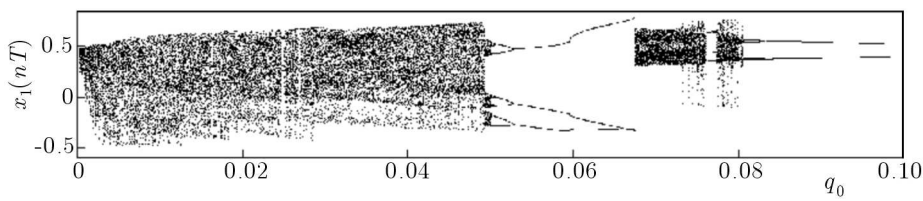

Fig. 6. Bifurcation diagram – influence of the parameter q_0 ($\varepsilon_1 = 0.1$, $\omega = 1$)

The influence of the parameter q_0 is also illustrated in the bifurcation diagram shown in Fig. 6. A cursory observation of the diagram shows that for $q_0 < 0.0508$ only chaotic vibrations are excited. However, analysing the diagram in more detail, it is possible to detect at least two very narrow ranges of periodic vibration (somewhat brighter trails in the neighbourhoods $q_0 = 0.0165$ and $q_0 = 0.025$). For $q_0 = 0.0164$, $4T$-periodic vibration takes place, whereas for $q_0 = 0.01645$ and $q_0 = 0.0165$ the period of oscillations is respectively equal to $8T$ and $12T$. In the range $0.02485 < q_0 < 0.025$, $3T$-periodic vibration is excited, which next for $q_0 = 0.0255$ gives place to $6T$-periodic vibration. For $q_0 = 0.047$, one can also observe $6T$-periodic vibrations.

Interesting is the fact that in the next ranges of chaotic vibrations lying between the ranges of sub-harmonic vibrations, the shape of the fractal undergoes a qualitative change (Fig. 7). For larger values of q_0 ($0.067 < q_0 < 0.08$),

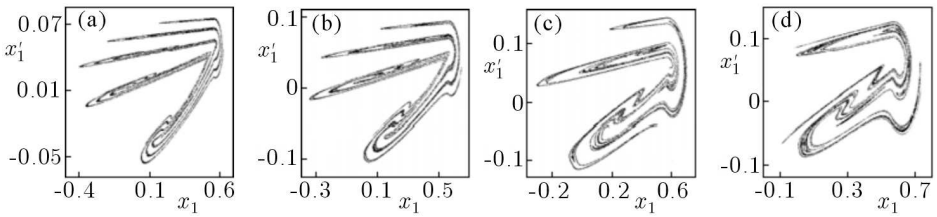

Fig. 7. Stroboscopic portraits of chaotic oscillations ($\varepsilon_1 = 0.1$, $\omega = 1$): (a) $q_0 = 0.014$, (b) $q_0 = 0.02$, (c) $q_0 = 0.04$, (d) $q_0 = 0.05$

the change of the shape of fractals is insignificant – they have a similar shape to the strange attractor shown in Fig. 7d.

Variation of the parameters χ_1 and χ_2 does not cause qualitative changes of the analysed diagram (Fig. 6) and stroboscopic portraits (Fig. 7). Even by assuming that the meshing stiffness is constant ($\chi_1 = \chi_2 = 0$), one can obtain similar results (Li *et al.*, 2001).

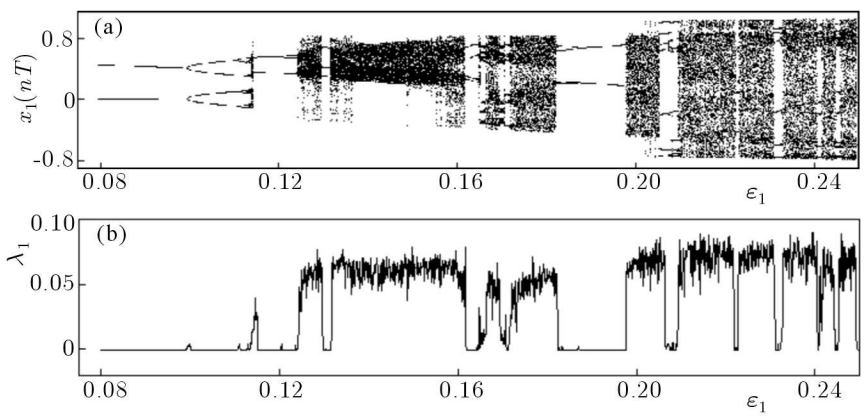

Fig. 8. Effect of the parameter ε_1 ($q_0 = 0.1$, $\omega = 1$): (a) bifurcation diagram, (b) diagram of maximal Lyapunov exponent

Figure 8 shows a bifurcation diagram and a corresponding diagram of the maximum Lyapunov exponent. The bifurcation diagram has been obtained using the stroboscopic method by taking the displacement x_1 at selected time instants (every excitation period). Both diagrams correspond to the section of the (ω, ε_1) plane shown in Fig. 2a taken for $\omega = 1$.

For larger amplitudes of the kinematic excitation, the probability of chaotic excitation is considerable. For this reason, other types of vibrations (except $2T$-periodic ones) are hardly observed in the regions of chaotic vibrations shown in Fig. 2a. Analysing the bifurcation diagram or the maximum Lyapunov exponent, one can more easily detect ranges of periodic vibration.

The bifurcation diagram contains more information than the Lyapunov exponent about the character of motion, enabling determination of the order of sub-harmonic vibration. The order of sub-harmonic oscillation is equal to the number of curves in the respective ranges of the parameter ε_1 (Fig. 8a). For example, in the case of $\varepsilon_1 = 0.206$ and $\varepsilon_1 = 0.208$, we have sub-harmonic vibration of 1:8 and 1:16 types, respectively. By preparing the diagram more precisely or analysing stroboscopic portraits, it is possible to show that for $\varepsilon_1 = 0.209$ vibration of the 1:32 type takes place. For sligth larger values of ε_1, chaotic vibrations are excited.

The differences between chaotic and sub-harmonic vibrations are not too big. This fact is confirmed by the similarity of some characteristics obtained for chaotic (Fig. 9a for $\varepsilon_1 = 0.23$) and sub-harmonic oscillations (Fig. 9b for $\varepsilon_1 = 0.231$). Analysing the frequency spectra (calculated by the FFT method) as well as the time histories, it is difficult to unambiguously determine the type of the analysed signal. Only by observing stroboscopic portraits it is possible to notice clear differences as well as to determine the order of sub-harmonic vibrations.

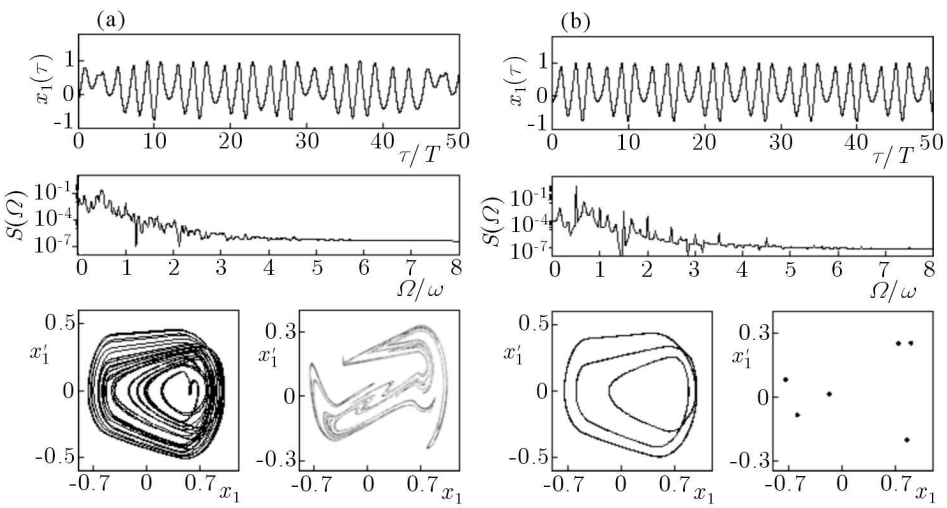

Fig. 9. Time histories, frequency spectra, phase trajectories and stroboscopic portraits: ($q_0 = 0.1$, $\omega = 1$): (a) $\varepsilon_1 = 0.23$, (b) $\varepsilon_1 = 0.231$

The results shown in Fig. 9a are typical for chaotic vibrations in a relatively wide frequency range and a broad range of the amplitude of kinematic excitations. Similar phase trajectories were obtained in the paper by Bonori and Pellicano (2007), who numerically analysed equation (2.17) for the case: $q_0 = 0.12$, $\omega = 1.7$, $\varepsilon_1 = 0.09$.

4. Influence of lateral vibrations on torsional ones

The numerical results discussed above do not undergo large qualitative changes after taking into account the stiffnesses of the supports. With this regard, below we demonstrate selected results, which illustrate perceptible tendencies of qualitative changes.

The full system of equations (2.12) describes now transverse and torsional vibrations. Additionally, the parameters μ_1, μ_2, κ_1, κ_2, ζ_1 and ζ_2 have the influence on the solutions to the set (2.12). To simplify the considerations, we further assume that the investigated system is symmetric, i.e. $\mu_1 = \mu_2 = 4$, $\kappa_1 = \kappa_2 = \kappa$ and $\zeta_1 = \zeta_2 = 0.01$.

Because in the case of sufficiently large stiffnesses of the supports of the gear wheels (for κ greater than about 20) it is difficult to observe essential differences in the results, we restrict the range of changes of the parameter κ to the interval $(0.2, 10)$.

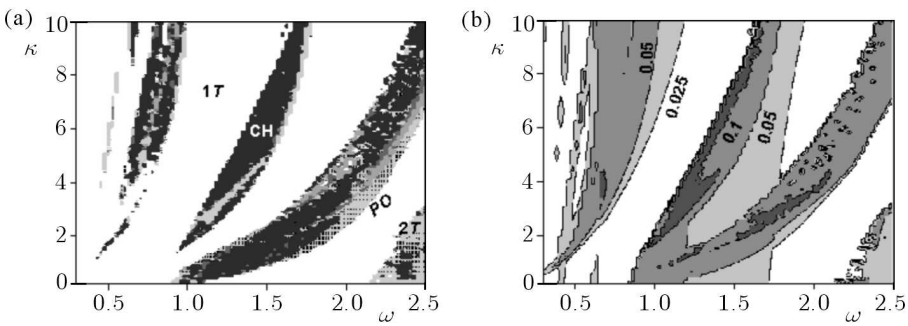

Fig. 10. Effect of the parameters ω and κ ($\varepsilon_1 = 0.05$, $q_0 = 0.1$, $\chi_0 = 0.25$, $\zeta = 0.025$): (a) vibration zones, (b) quality index

Figure 10 illustrates the effect of the parameters ω and κ on the type of vibrations (Fig. 10a) as well as on the rms value of velocity x_1' (Fig. 10b). The regions of chaotic and periodic vibrations appear alternately, whereas the chaotic regions partly overlap the regions of the raised level of vibrations. With increasing the non-dimensional stiffness κ, the ranges of chaotic oscillations displace toward higher frequency ranges. Moreover, one can observe a new type of vibrations – quasi-periodic, discussed below in more detail.

In order to compare the present results with earlier presented in Fig. 2 we investigate the effect of parameters ω and ε_1 (Fig. 11) for a prescribed, comparatively small, value of the parameter $\kappa = 0.5$.

The analysis of the results shows some insignificant differences. We have similar regions, but shifted to the right with respect to the previous re-

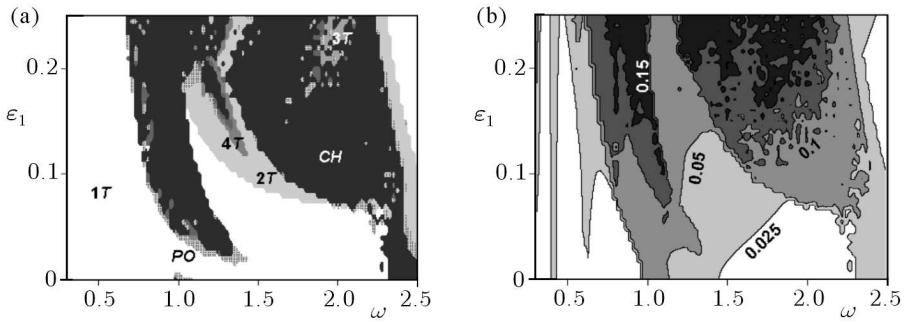

Fig. 11. Effect of the parameters ω and ε_1 ($\kappa = 0.5$, $q_0 = 0.1$, $\chi_0 = 0.25$, $\zeta = 0.025$): (a) vibration zones, (b) quality index

gions. Moreover, in Fig. 11a in the neighbourhood of $\omega = 1$, there appears an additional region of chaotic vibration, rimmed through the narrow zones of quasi-periodic and sub-harmonic oscillations of a higher order.

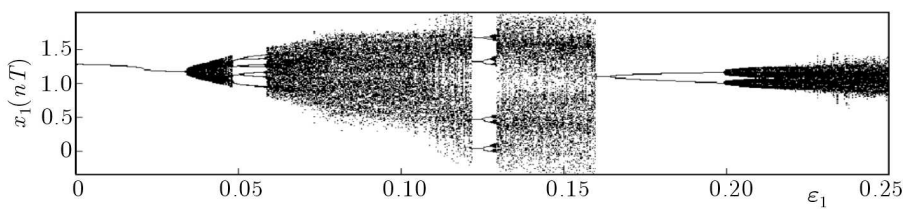

Fig. 12. Bifurcation diagram – influence of the parameter ε_1 ($\kappa = 0.5$, $q_0 = 0.1$, $\omega = 1.05$)

In Fig. 12, a bifurcation diagram that corresponds to the sections of Fig. 11a for $\omega = 1.05$ is shown. Quasi-periodic vibrations are excited for the amplitude ε_1, contained in the interval $(0.033, 0.048)$ as well as for $\varepsilon_1 > 0.2$.

In the first range of the parameter ε_1, quasi-periodic solutions are created from periodic solutions – the stroboscopic portrait is a single closed curve (Fig. 13a). In the second range, for $\varepsilon_1 > 0.2$, $2T$-periodic solutions change into quasi-periodic, and two closed curves make the stroboscopic portrait (Fig. 13b).

In general, quasi-periodic vibrations have somewhat smaller amplitudes in relation to chaotic vibration, which is partly visible on the bifurcation diagram. It should be pointed out that in the discussed ranges of the parameter ?1 other types of vibrations are also possible, though probability of them to be excited is considerably smaller than in the remaining ranges.

Earlier, Raghothama and Narayanan (1999) detected quasi-periodic vibration by analysing a model of a gearbox with flexible supports.

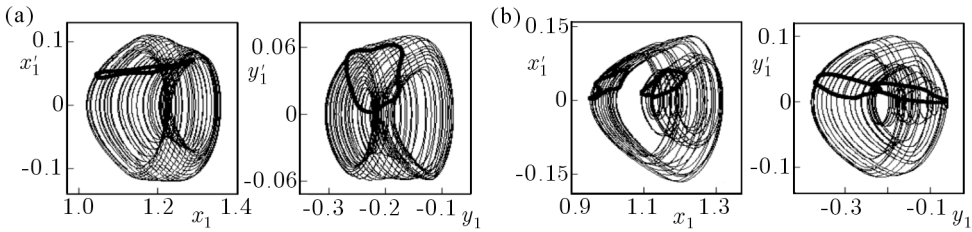

Fig. 13. Phase trajectories and stroboscopic portraits ($\kappa = 0.5$, $q_0 = 0.1$, $\omega = 1.05$): (a) $\varepsilon_1 = 0.04$, (b) $\varepsilon_1 = 0.205$

Analogous conclusions relating to the character of vibration can be drawn from the analysis of diagrams shown in Fig. 14, which illustrate the influence of the nondimensional moment q_0. In the ranges of quasi-periodic vibrations, the stroboscopic points are usually distributed more regularly – this remark concerns the interval $(0.13, 0.17)$ in Fig. 14a as well as the interval $(0.16, 0.18)$ in Fig. 14b.

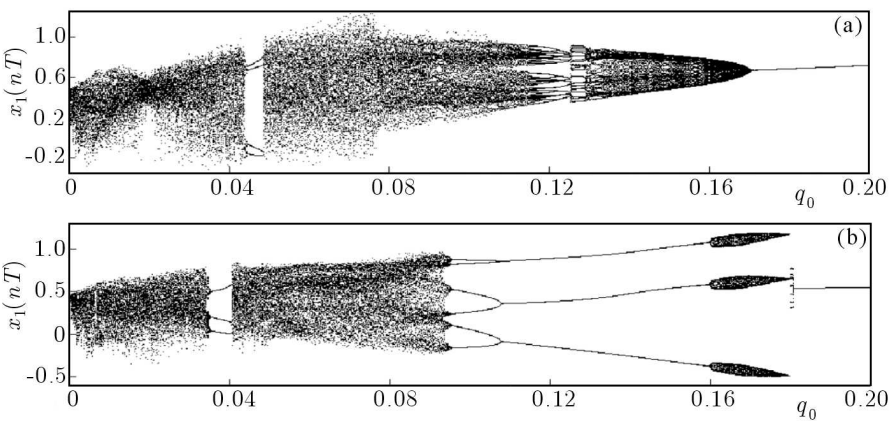

Fig. 14. Bifurcation diagram – influence of the parameter q_0 ($\varepsilon_1 = 0.1$, $\omega = 1.05$): (a) $\kappa = 0.5$, $\omega = 0.9$, (b) $\kappa = 1$, $\omega = 1$

Both diagrams can be compared with that earlier shown in Fig. 6. One can easily observe that the zone of chaotic vibration with regard to transverse motion becomes wider. It should be noted that the range of changes of q_0 is twice as large as now than that in Fig. 6. The character of chaotic and quasi-periodic motion is similar. This is confirmed by the similarity of stroboscopic portraits obtained for chaotic (Fig. 15a) and quasi-periodic oscillations (Fig. 15b).

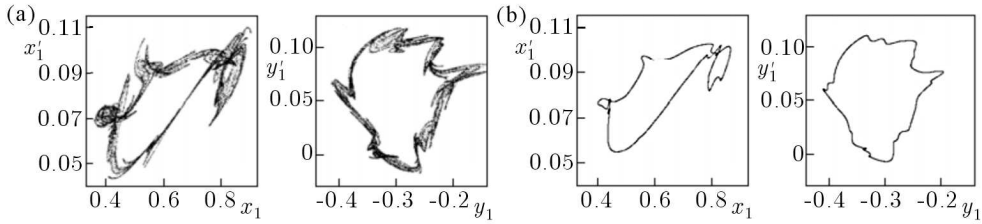

Fig. 15. Stroboscopic portraits ($\kappa = 0.5$, $\omega = 0.9$, $\varepsilon_1 = 0.1$): (a) $q_0 = 0.128$, (b) $q_0 = 0.135$

5. Conclusions

Detailed conclusions have been successively drawn in the discussion of the results of numerical calculations. The most important conclusions can be summarized as follows:

- The analysis of the effect of parameters on the character of vibration and the introduced quality index enable one to determine ranges of the parameters, for which vibration amplitudes are sufficiently small. Higher levels of vibration are observed in the low frequency range (for $\omega < 2$), mainly in regions of parametric resonance (in the neighbourhood of points $\omega = 1/4$, $\omega = 1/2$, $\omega = 1$ and $\omega = 2$). In these regions, apart from the rotational speed, the parameters of parametric excitations play an important role.

- The investigation of the character of motion is interesting mainly from the cognitive point of view. The parameters of the kinematic excitation as well as the static load torque have the decisive influence on the type of oscillations. However, since a raised level of oscillation is usually observed in chaotic regions, it is possible to use the results of qualitative analysis for selection of parameters of the gear transmission system.

- For small values of the nondimensional static load, the solutions to differential equations strongly depend on the initial conditions. We can have different types of subharmonic and chaotic vibrations, considerably differing in the amplitude of oscillation.

- The taking into account the stiffnesses of the gearbox supports results in growth of the ranges of chaotic oscillations. Moreover, a new type of oscillation – quasi-periodic vibration – gets excited in the system.

- By analysing the model of the system, it is possible to observe different scenarios of generation of chaotic oscillations. They can come into existence both from sub-harmonic oscillations as well as quasi-periodic vibrations.

References

1. Bonori G., Pellicano F., 2007, Non-smooth dynamics of spur gears with manufacturing errors, *Journal of Sound and Vibration*, **306**, 271-283
2. De Souza S.L.T., Caldas I.L., Viana R.L., Balthazar J.M., 2004, Sudden changes in chaotic attractors and transient basins in a model for rattling in gearboxes, *Chaos, Solitons and Fractals*, **21**, 763-772
3. Dyk J., Krupa A., Osiński J., 1994, Analysis of chaos in systems with gears, *Mechanika Teoretyczna i Stosowana*, **32**, 3, 549-563
4. Gill-Jeong C., 2007, Nonlinear behavior analysis of spur gear pairs with a one-way clutch, *Journal of Sound and Vibration*, **304**, 18-30
5. Li Y., Zheng L., Mi L., 2001, Bifurcation and chaotic motion of a piecewise linear vibration system in gear-pairs, *International Journal of Gearing and Transmissions*, **3**, 126-133
6. Litak G., Friswell M.I., 2003, Vibration in gear systems, *Chaos, Solitons and Fractals*, **16**, 795-800
7. Łuczko J., 2006, Numerical methods of determining the regions of subharmonic and chaotic vibrations, *Czasopismo Techniczne*, **11-M**, 39-62 [in Polish]
8. Müller L., 1986, *Tooth Gears: Dynamics*, WNT, Warszawa [in Polish]
9. Raghothama A., Narayanan S., 1999, Bifurcation and chaos in geared rotor bearing system by incremental harmonic balance method, *Journal of Sound and Vibration*, **226**, 3, 469-492
10. Shen Y., Yang S., Liu X., 2006, Nonlinear dynamics of a spur gear pair with time-varying stiffness and backlash based on incremental harmonic balance method, *International Journal of Mechanical Sciences*, **48**, 1256-1263
11. Theodossiades S., Natsiavas S., 2001, Periodic and chaotic dynamics of motor-driven gear-pair systems with backlash, *Chaos, Solitons and Fractals*, **12**, 2427-2440
12. Vaishya M., Singh R., 2001, Analysis of periodically varying gear mesh systems with Coulomb friction using Floquet theory, *Journal of Sound and Vibration*, **243**, 3, 525-545

Drgania chaotyczne w przekładniach zębatych

Streszczenie

W pracy przeprowadzono analizę jakościową modelu jednostopniowej przekładni zębatej. Uwzględniono wpływ zmiany sztywności zazębienia, luzu międzyzębnego oraz wymuszeń kinematycznych. Do analizy wykorzystano procedury numerycznego całkowania skojarzone z algorytmami szybkiej transformaty Fouriera. Zbadano wpływ parametrów układu na charakter drgań oraz wprowadzone wskaźniki jakości. Wykazano możliwość generowania się w badanym układzie drgań chaotycznych, prawie okresowych i podharmonicznych.

Manuscript received March 19, 2008; accepted for print July 3, 2008